

SUPPLEMENTARY MATERIAL

**A sporadic Alzheimer's blood-brain barrier model for developing
ultrasound-mediated delivery of Aducanumab and anti-Tau antibodies**

Wasielewska *et al.*

SUPPLEMENTAL FIGURES

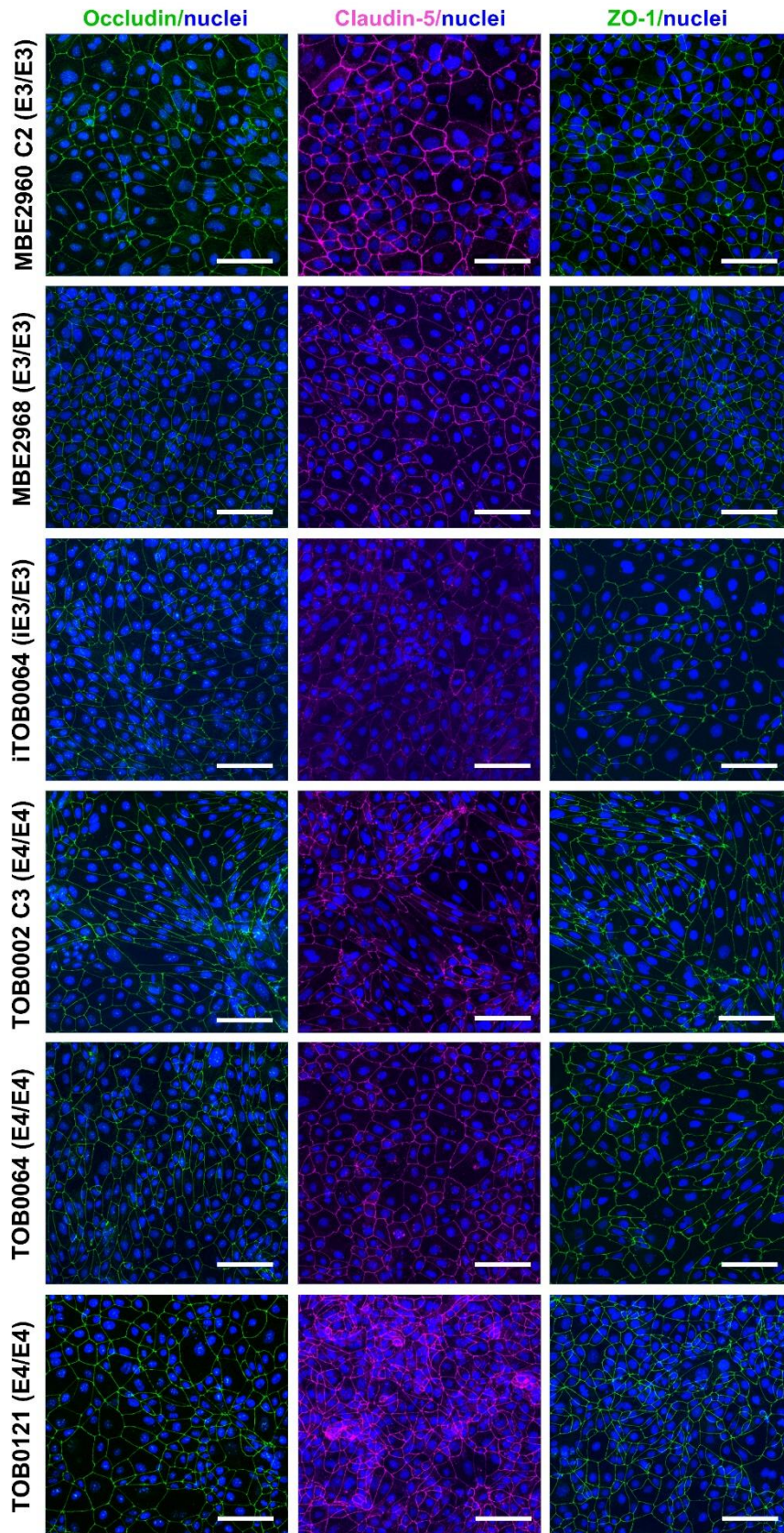


Figure S1. Characterization of iBECs generated from individual iPSC lines. Immunofluorescence images of occludin (green), claudin-5 (magenta) and ZO-1 (green) in

iBECs generated from *APOE3* and *APOE4* induced pluripotent stem cells (iPSCs) used in this study. Hoechst counterstain, scale bar = 100 μm .

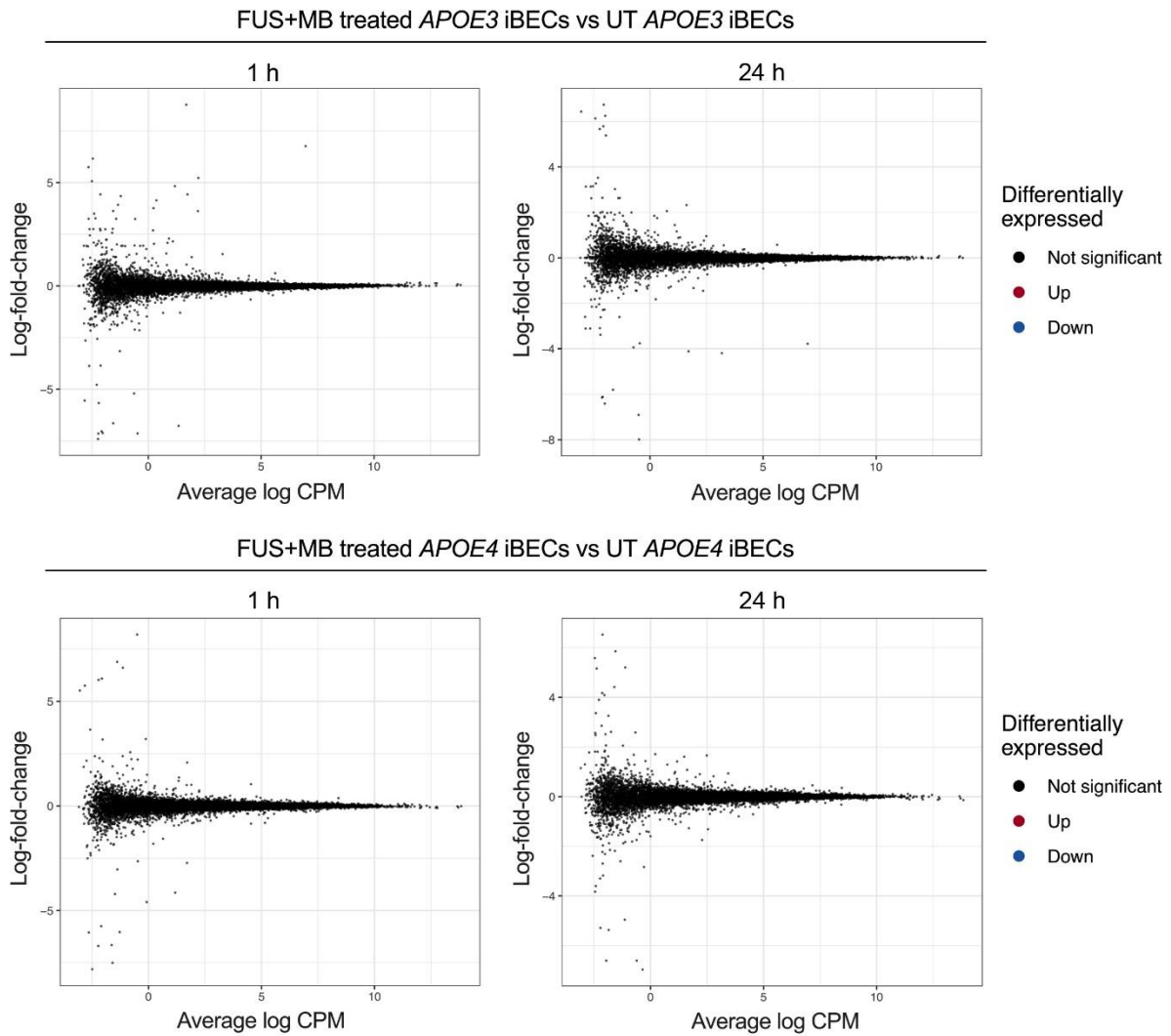


Figure S2. Differential expression analysis of FUS^{+MB} treated iBEC vs untreated iBECs at 1 h and 24 h for *APOE3* and *APOE4* genotypes. Mean-difference (MD) plots showing log-fold-change versus average log expression values (log₂ counts per million, CPM). Upper panel: FUS^{+MB} treated *APOE3* iBECs at 1 h vs untreated (UT) *APOE3* iBECs at 1 h and FUS^{+MB} treated *APOE3* iBECs at 24 h vs UT *APOE3* iBECs at 24 h. Lower panel: FUS^{+MB} treated *APOE4* iBECs at 1 h vs UT *APOE4* iBECs at 1 h and FUS^{+MB} treated *APOE4* iBECs at 24 h vs UT *APOE4* iBECs at 24 h.

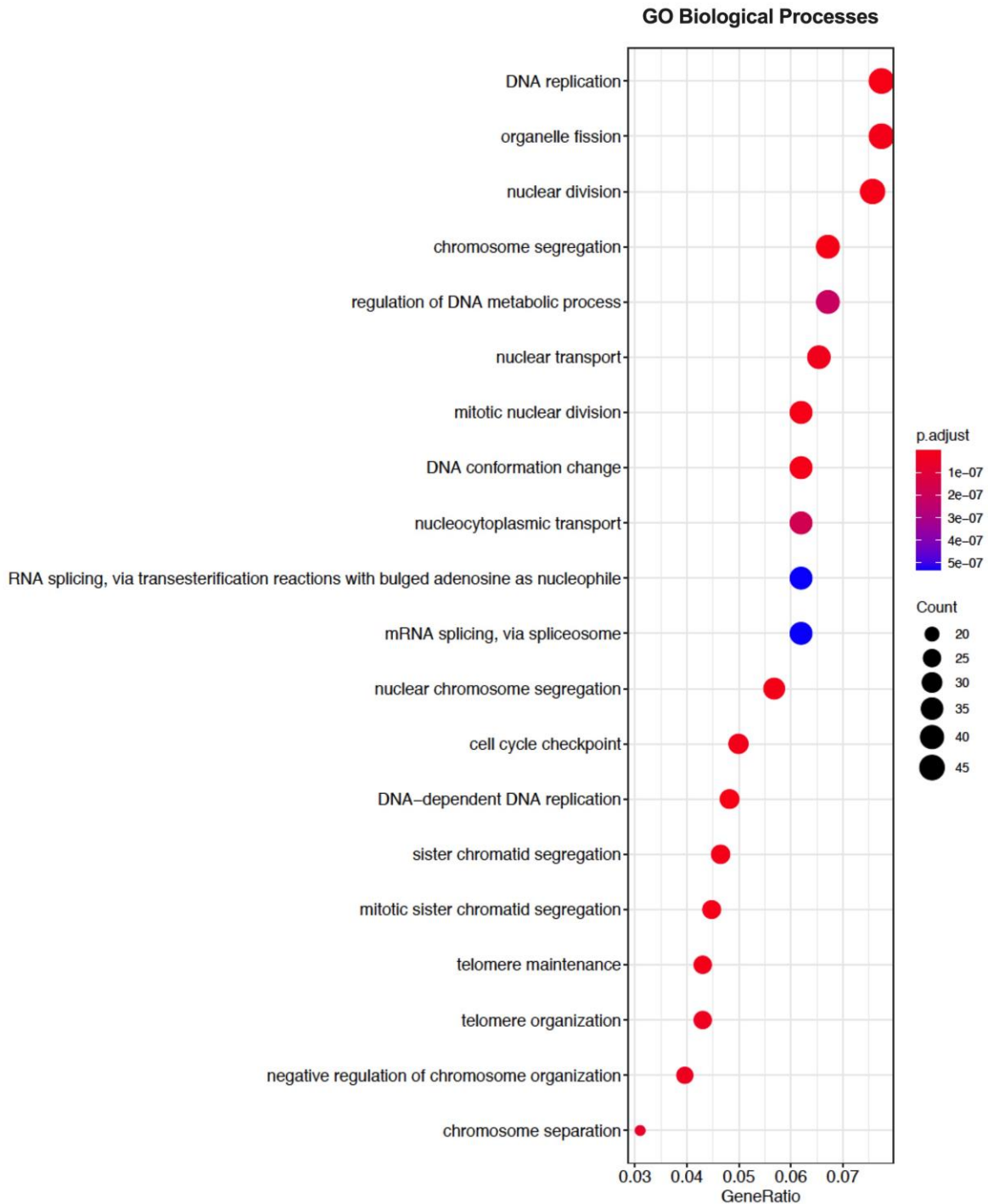


Figure S3. Dotplot of top gene ontology (GO) terms from sub ontology Biological Process enriched from comparison of UT *APOE4* iBECs at 1 h vs *APOE3* iBECs at 1 h. The top 20 GO processes according to *P*-value plotted in order of gene ratio. The size of the dots represents the number of genes associated with the GO term and the color of the dots represent the *P*-adjusted values. The differentially expressed genes (FDR < 0.05) were used for analysis.

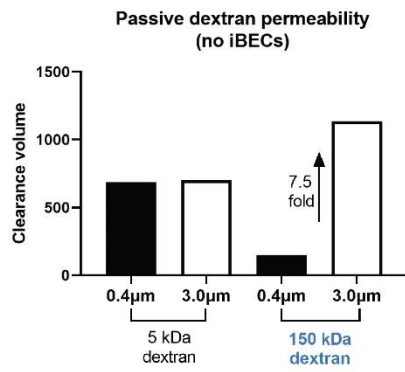
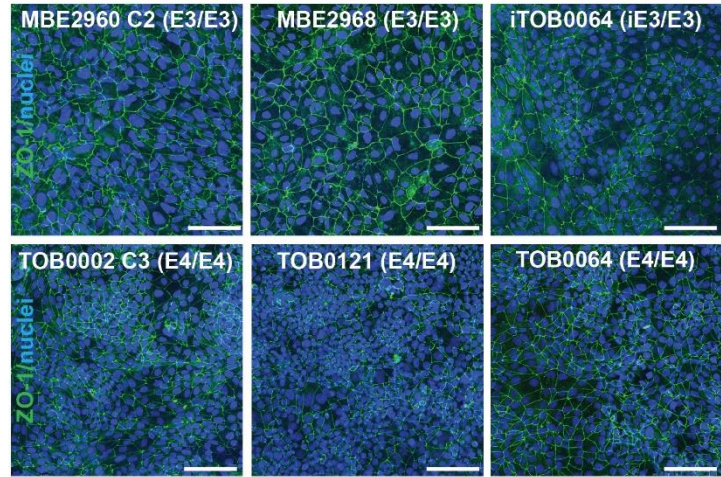
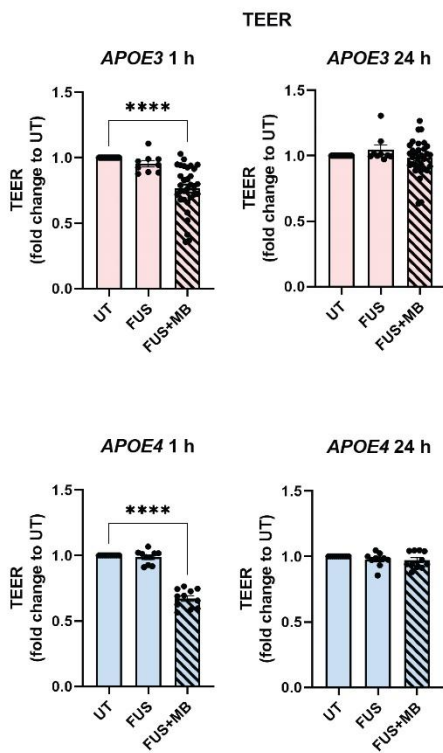
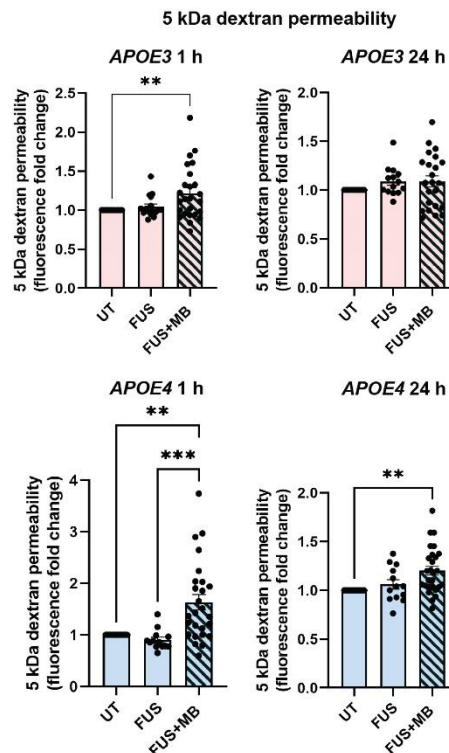
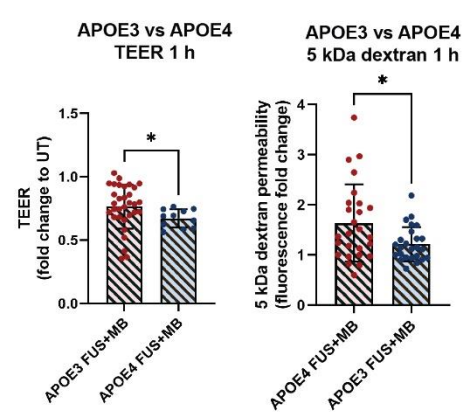
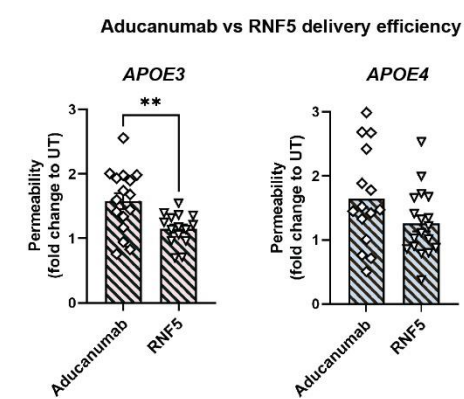
A**B****C****D****E****F**

Figure S4. Optimization of the Ø 3.0 µm pore Transwell model and characterization of the effects of FUS^{only} and FUS^{+MB} on iBECs. (A) Passive permeability (clearance volume) of 5 kDa and 150 kDa dextran in collagen IV and fibronectin coated (no iBEC containing) Ø 0.4 µm and Ø 3.0 µm pore Transwell inserts. (B) Immunofluorescence of ZO-1 (green) in each individual *APOE3* and *APOE4* iBEC line seeded on Ø 3.0 µm pore Transwell inserts (Hoechst counterstain, scale bar = 100 µm). (C) Trans-endothelial electrical resistance (TEER, fold change to untreated (UT)) in *APOE3* and *APOE4* iBECs in UT, FUS^{only} and FUS^{+MB} conditions at 1 h and 24 h following treatment (N = 2 biological replicates and a minimum of n = 3 independent replicates per line). (D) 5 kDa dextran permeability (fluorescence fold change to UT) in *APOE3* and *APOE4* iBECs in UT, FUS^{only} and FUS^{+MB} conditions at 1 h and 24 h following treatment (N = 2 biological replicates and a minimum of n = 3 independent replicates per line). (E) Comparison of TEER and 5 kDa dextran permeability following FUS^{+MB} between *APOE3* and *APOE4* iBECs (permeability shown as relative values to UT at 1 h). (F) Comparison of Aducanumab-analogue and RNF5 delivery efficiency following FUS^{+MB} in *APOE3* and *APOE4* iBECs (permeability shown as relative values to UT at 24 h). Error bars = SEM. * $P < 0.05$, ** $P < 0.01$, *** $P < 0.001$ and **** $P < 0.0001$ by one-way ANOVA for graphs with three groups and by Unpaired t-test with Welch's correction for graphs with two groups.

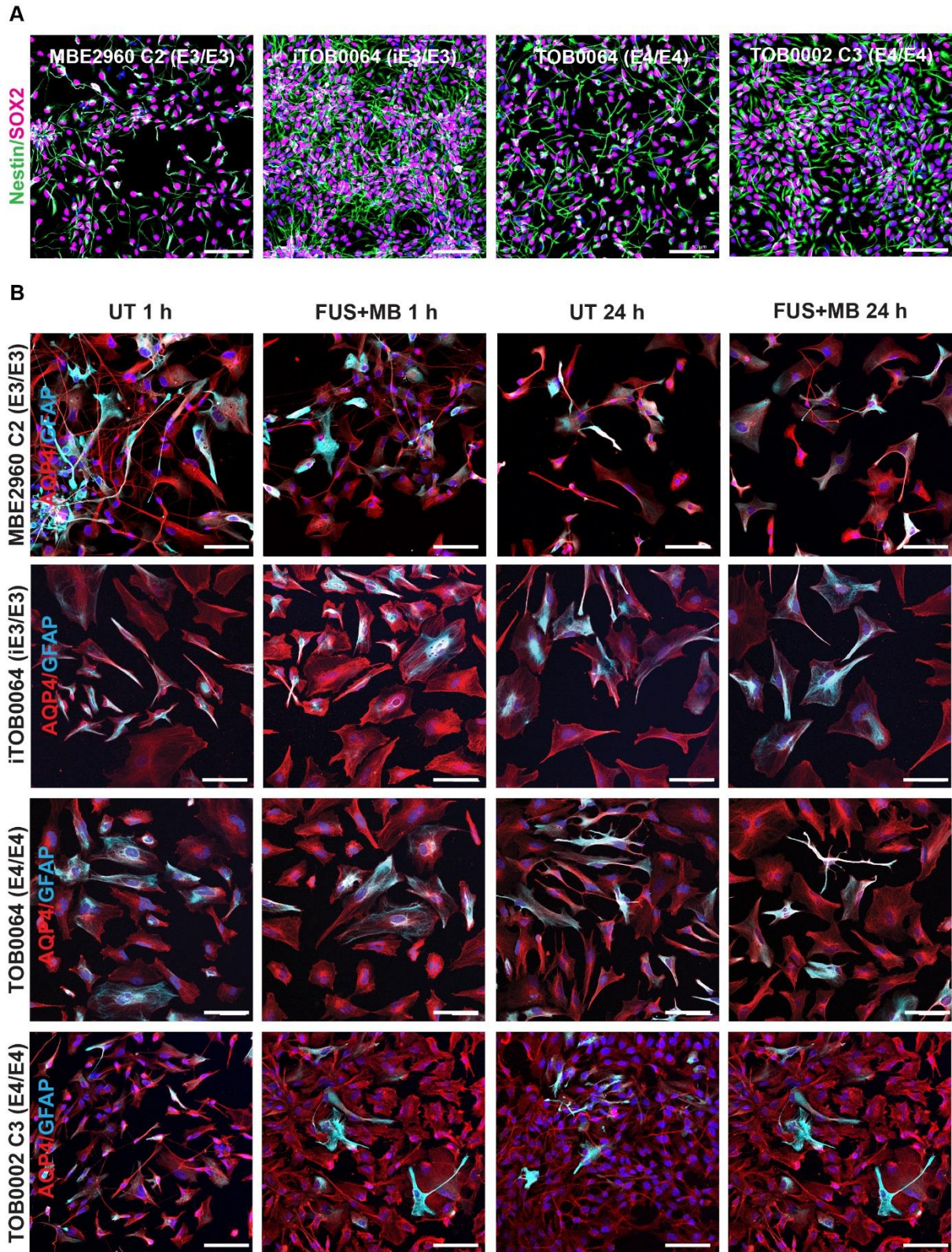


Figure S5. Neural progenitor cell generation and FUS^{+MB} treatment of iAstrocytes. (A) Immunofluorescence of nestin (green) and SOX2 (magenta) in neural progenitor cells (NPCs) generated from *APOE3* and *APOE4* induced pluripotent stem cells (iPSCs) used in this study. (B) Immunofluorescence of *APOE3* and *APOE4* iAstrocytes generated from individual iPSC

lines in untreated (UT) and focused ultrasound + microbubble (FUS^{+MB}) conditions 1 h and 24 h following treatment stained with AQP4 (red) and GFAP (cyan) (Hoechst counterstain, scale bar = 100 μm).

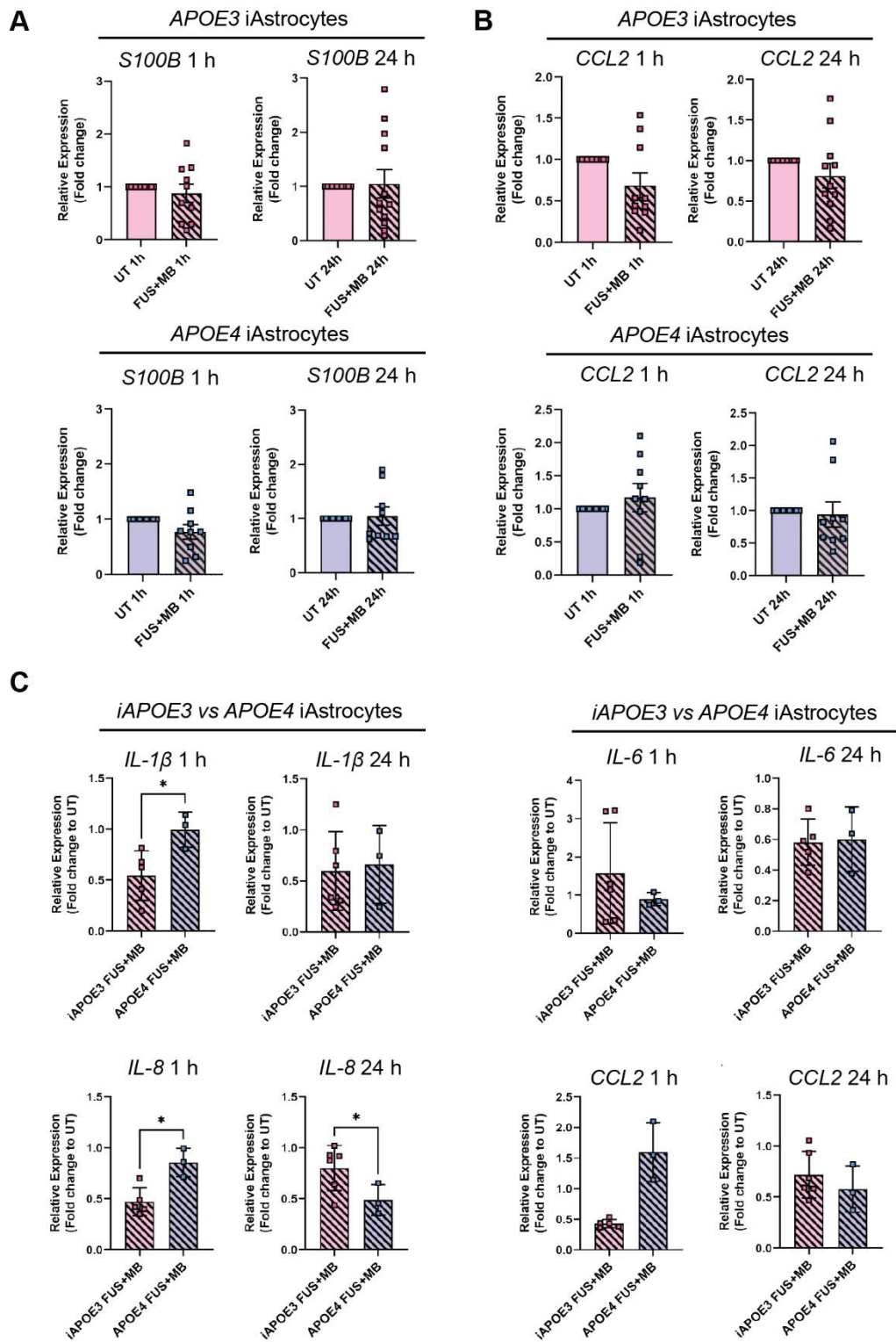


Figure S6. Effect of FUS^{+MB} on iAstrocyte gene expression. Relative gene expression (fold change) of (A) astrocyte marker *S100B* and (B) inflammatory cytokine *CCL2* in UT and FUS^{+MB} treated *APOE3* and *APOE4* iAstrocytes 1 h and 24 h after treatment, error bars = SEM. (C) Comparison of relative gene expression (fold change) of inflammatory markers between

an isogenic *iAPOE3* and *APOE4* iAstrocyte pair at 1 h and 24 h after FUS^{+MB} treatment, error bars = SD. * $P < 0.05$ by Unpaired t-test with Welch's correction.

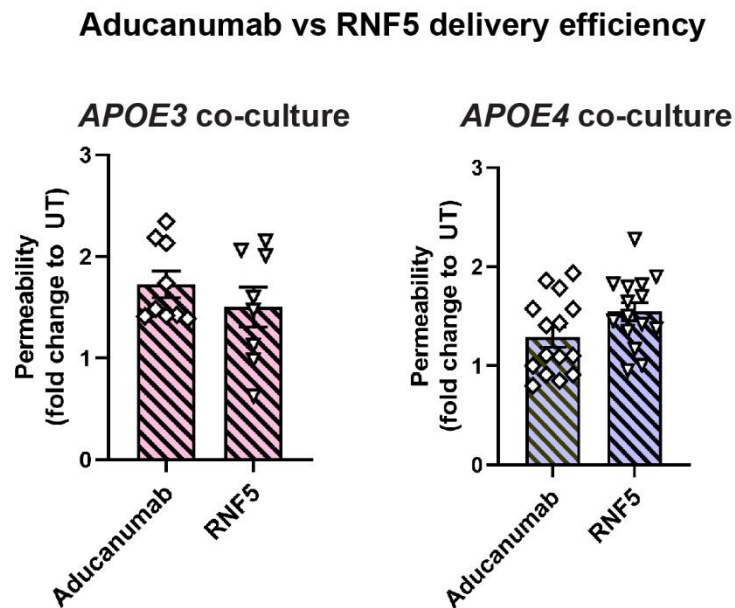


Figure S7. Comparison of Aducanumab-analogue and RNF5 delivery efficiency following FUS^{+MB} in *APOE3* and *APOE4* co-cultures. Aducanumab and RNF5 delivery efficiency following FUS^{+MB} in *APOE3* and *APOE4* iBEC and iAstrocyte co-cultures (permeability shown as relative values to UT at 24 h).

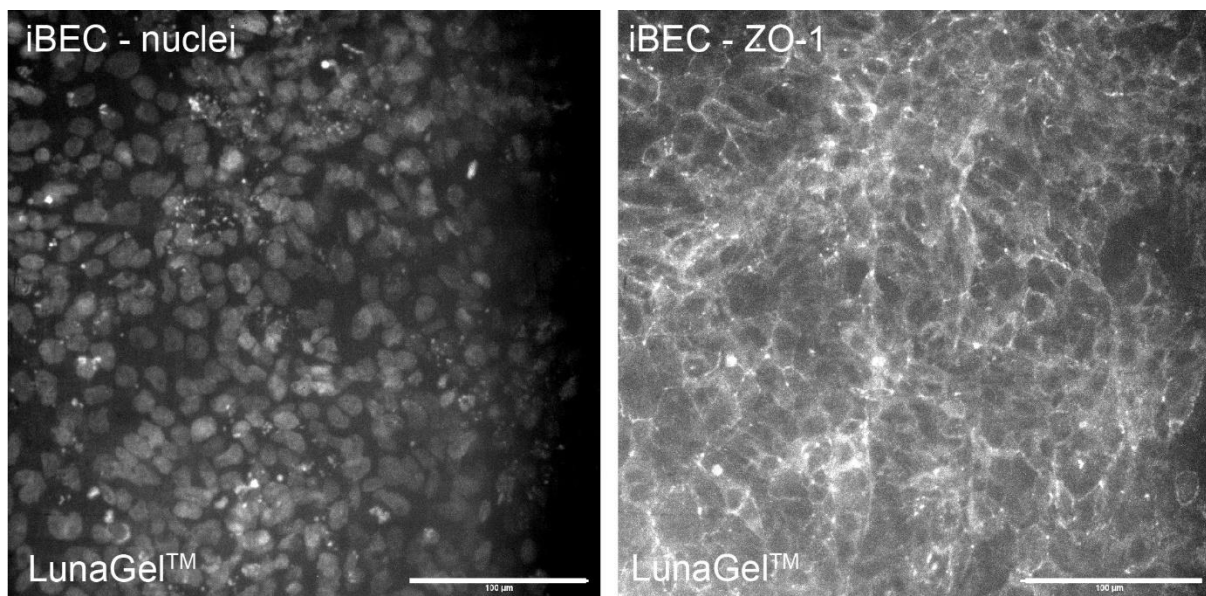


Figure S8. iBEC barrier formation on LunaGel™. Greyscale images of Hoechst staining (left panel) and ZO-1 staining (right panel) in iBECs seeded on LunaGel™ (scale bar = 100 µm).

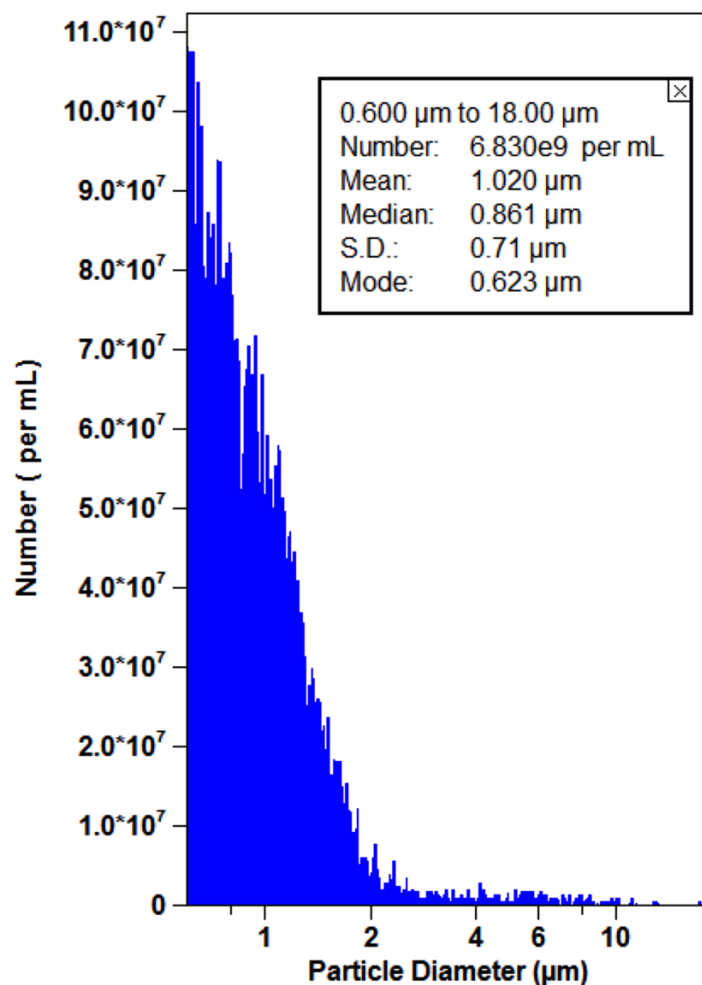


Figure S9. Characterization of microbubbles used in the study. Representative size and distribution profiles of in-house prepared gas-filled microbubbles measured with a Coulter counter. The average diameter of microbubbles used in the study was $1.24 \pm 0.31 \mu\text{m}$, with a concentration of $7.47 \pm 6.06 \times 10^9$ MBs/ml ($n = 6$ MB vials analysed).

SUPPLEMENTAL TABLES

Table S1. Results from differential expression analysis of UT *APOE4* iBECs compared to UT *APOE3* iBECs at 1 h. Genes sorted by *P*-value. Differentially expressed genes (DEGs) defined by FDR < 0.05.

Table can be found in .xlsx format

Table S2. Results from gene ontology (GO) enrichment analysis of sub ontology Biological Process from comparison of UT *APOE4* iBECs at 1 h vs *APOE3* iBECs at 1 h.

Table can be found in .xlsx format

Table S3. Primer sequences used in the study.

Target gene	Forward primer sequence	Reverse primer sequence
Ve-cadherin (<i>CDH5</i>)	AGGCAAGATCAAGTCAA GCGT	GAGTCTCCAGGTTTTCGC CA
Claudin-5 (<i>CLDN5</i>)	GATTGAGAGGTCTGGGA AGCC	ATCCCATGGCAAACAGA GAGG
Occludin (<i>OCLN</i>)	GAAGCAAGTGAAGGGAT CTGC	ACAACCTGGCATCAGCC TTCT
Zonula occludens-1 (<i>TJP-1</i>)	ACAGCTACAGGAAAATG ACCGA	ACTGGTTCAGGATCAGG ACG
<i>SOX18</i>	TCAGCAAGATGCTGGGC AAAG	GCGGCCGGTACTTGTAG TTG
Interleukin-6 (<i>IL-6</i>)	TGCAATAACCACCCCTG ACC	TGCGCAGAATGAGATGA GTTG
Interleukin-8 (<i>IL-8</i>)	AGACAGCAGAGCACACA AGC	ATGGTTCCTTCCGGTGGT
Interleukin-1 β (<i>IL-1β</i>)	AATCTGTACCTGTCCTGC GTGTT	TGGGTAATTTTTGGGATC TACACTCT
C-C motif chemokine ligand 2 (<i>CCL2</i>)	GTCATAGCAGCCACCTT CATT	GGACACTTGCTGCTGGT GATT
Glial fibrillary acidic protein (<i>GFAP</i>)	GAGGTTGAGAGGGACAA TCTGG	GTGGCTTCATCTGCTTCC TGTC
Aquaporin-4 (<i>AQP-4</i>)	GTAGTCACCATGGTTCAT GGAAAT	TGGAACACAGCTGGCAA AGA
S100 calcium-binding protein β (<i>S100β</i>)	TTCTGGAAGGGAGGGAG ACA	CTCCTGCTCTTTGATTTC CTCT
<i>18S</i>	TTCGAGGCCCTGTAATTG GA	GCAGCAACTTTAATATA CGCTATTGG

Table S4. Antibodies used in the study.

Primary antibodies	Species	Source	Identifier
ZO-1	mouse	Invitrogen	Cat# 339100
occludin	rabbit	Invitrogen	Cat# 711500
claudin-5	mouse	Invitrogen	Cat# 352500
aquaporin-4	mouse	Abcam	Cat# ab9512
GFAP	rabbit	Agilent/ Dako	Cat# Z0334
nestin	mouse	Abcam	Cat# ab22035
SOX2	rat	Invitrogen	Cat# 14981182
Secondary antibodies			
Secondary antibodies	Species	Source	Identifier
anti-mouse Alexa Fluor 488	goat	Invitrogen	Cat# A11029
anti-mouse Alexa Fluor 594	goat	Invitrogen	Cat# A11032
anti-mouse Alexa Fluor 647	goat	Invitrogen	Cat# A32728
anti-rabbit Alexa Fluor 488	goat	Invitrogen	Cat# A11034
anti-rat Alexa Fluor 647	goat	Invitrogen	Cat# A21247